FEBS Letters 345 (1994) 193–197

FEBS 14066

Isolation, primary structures and metal binding properties of neuronal growth inhibitory factor (GIF) from bovine and equine brain

Dean L. Pountney, Sibylle M. Fundel, Peter Faller, Neil E. Birchler, Peter Hunziker, Milan Vašák*

Biochemisches Institut der Universität Zürich, Winterthurerstrasse 190, 8057 Zürich, Switzerland

Received 16 March 1994; revised version received 21 April 1994

Abstract

Human neuronal growth inhibitory factor (GIF) impairs the survival of cultured neurons and is deficient in the brains of Alzheimer's disease victims. We have isolated and sequenced analogous proteins from bovine and equine brain. By comparing their primary structures with those of human, mouse and rat GIFs, a consensus GIF sequence was obtained. Although this exhibits ca. 65% similarity with primary structures of mammalian metallothioneins (MTs), some significant differences are expected in the content of helix and turn secondary structures. In contrast to MTs, which usually bind 7 Zn(II) ions, human, bovine and equine GIFs contain 1–4 Cu(I) and 3–5 Zn(II) ions in species-specific ratios. The observed Cu(I) phosphorescence (λ_{max}, 550–590 nm; τ, 100 μs at 77 K) indicates the presence of the cuprous ion. Both bovine Cu_1Cd_5- and the equine Cu_3Cd_3-GIF derivatives (Cd replacing Zn) exhibit cadmium-dependent absorption and CD features between 220–260 nm characteristic of Cd-thiolate clusters similar to those in Cd-MTs.

Key words: Alzheimer's Disease; Cd substitution; CysS-Cd(II) LMCT; Cu(I)-thiolate; Neuronal growth; Metallothionein; Cu(I) phosphorescence; Exciton coupling; Cadmium-thiolate cluster

1. Introduction

Recently, a ~7 kDa protein has been isolated from normal human brain which is capable of inhibiting neuronal growth and survival in cell culture and which is deficient in the brains of Alzheimer's disease victims. Subsequent characterization of this growth inhibitory factor (GIF) revealed a metalloprotein of 68 amino acids containing four copper and three zinc ions [1]. The amino acid sequence of human GIF exhibits about 70% sequence similarity with those of mammalian metallothioneins (MTs) including the preserved array of 20 Cys [2,3]. Furthermore, the GIF gene has a similar intron/exon structure to that of MT (MT-1 and MT-2) leading to its classification as MT-3 [4]. Relative to mammalian MTs (normally 61 amino acids), GIF contains two conserved inserts of a single Thr and a Glu-rich hexapeptide in the N-terminal and C-terminal regions, respectively [1,4,5]. Their biological properties also differ. In contrast to MTs, which are predominantly expressed in parenchymatous tissues, GIF is found exclusively in the brain. Furthermore, GIF mRNA levels were unaffected by the administration of heavy metal ions and other potent inducers of MT biosynthesis [4] and in neuronal cell culture studies MTs do not exhibit neuronal growth inhibitory activity [1].

Previously metal ions have been found to influence the polypeptide fold of the mammalian MTs [6–8]. Human GIF expressed in *E. coli* exhibits a greatly reduced biological activity (ca. 10%) compared with that of the native Cu,Zn-protein [9]. As in MT expression systems [10], this protein obtained in zinc-culture [11] would contain only zinc ions. The aim of the present study is to learn more about the structural features of native GIF focusing primarily on the mode of metal-binding.

2. Materials and methods

Isolation and purification of GIFs from bovine and equine brain were essentially the same as those for human brain [1], with the addition of an initial batch anion-exchange step (DEAE Sephacel, Pharmacia) before the gel permeation (Sephadex G-50) and anion-exchange (DEAE Sephacel) chromatographic procedures. The Cu,Cd-GIF derivatives were prepared by addition of $CdSO_4$ (80 μM) to the crude extracts.

2.1. Determination of amino acid sequence

Bound metal ions were removed from GIF with the chelating agent diethyldithiocarbamate (DTC) as in [12]. The Cys residues of the apoprotein were S-methylated as in [13]. Molecular masses of the apoproteins were determined by electrospray mass spectrometry using a Sciex API III triple-quadrupole instrument. For N-terminal sequencing by Edman degradation, the Ac-Met-Asp dipeptide was removed by acid-cleavage of the S-methylated proteins in 0.1% TFA as in [14]. Samples (2–5 nmol) of the S-methylated proteins were digested with trypsin (Boehringer; 2% w/w enzyme/substrate in 0.2 M *N*-methylmorpholine trifluoroacetate, pH 8.3, 30 min at 37°C). Peptides were purified by RP-HPLC (Aquapore RP-300 column, Brownlee Labs) using a 0.1% TFA/acetonitrile gradient system and their masses determined by electrospray mass spectrometry.

*Corresponding author. Fax: (41) (1) 363 7947.

Abbreviations: LMCT, ligand-to-metal charge transfer; DTC, diethyldithiocarbamate; GIF, neuronal growth inhibitory factor; Me(II), divalent metal ion; MT, metallothionein; CD, circular dichroism; RP-HPLC, reverse-phase high-performance liquid chromatography.

SSDI 0014-5793(94)00452-2

The amino acid compositions of the apoproteins, S-methylated proteins and tryptic peptides were determined using either an Applied Biosystems Inc. (model 420 A/H) or a Hewlett-Packard AminoQuant amino acid analyzer. The amino acid sequences of the chemically cleaved S-methylated proteins (1000 pmol) and of the tryptic peptides (500–1000 pmol) were determined using either a model 470A/900A or a model 477A protein/peptide sequencer, both equipped with model 120-A on-line amino acid analyzers (all Applied Biosystems Inc.). The relative sequence positions of the tryptic peptides were deduced according to their homology with the mouse (mGIF), rat (r-GIF) and human (h-GIF) GIF sequences. The C-terminal pentapeptide was confirmed by amino acid analysis upon timed enzymatic digestion of the S-methylated proteins with carboxypeptidase P (Boeringer). The partial sequence of the blocked N-terminal tryptic peptide of b-GIF was determined by tandem quadrupole mass spectrometry [15].

2.2. Protein characterization

Analytical gel filtration (FPLC) was performed using a Superdex 75 column (Pharmacia). Protein purity was checked by non-denaturing- and SDS-PAGE (12%) (Bio-Rad MiniProtean II). The ratio of bound metal ions to protein was determined using atomic absorption spectroscopy (IL Video 12) and quantitative amino acid analysis. The growth inhibitory activities of the native Cu,Zn-GIFs were assessed against slice cultures of rat hippocampus, prepared as described in [16].

Absorption spectra were recorded using either a Cary (model 3) or a Hitachi 380 spectrophotometer. Circular dichroism (CD) measurements were made using a Jasco (model J-500C) spectropolarimeter. Gaussian analysis of the difference absorption data was performed using the programme Peakfit (Jandel). Luminescence spectra at 77 K and decay data were obtained using a SPEX fluorolog spectrofluorimeter fitted with the 1934C phosphorimeter accessory. For low-temperature luminescence measurements, samples were contained in 2 mm i.d. stoppered quartz tubes and immersed in a cylindrical quartz Dewar vessel filled with liquid nitrogen. The absorption and CD spectra are referenced to the protein concentrations determined by quantitative amino acid analysis.

3. Results and discussion

3.1. Chemical characterization of GIF

Bovine GIF (b-GIF) and equine GIF (e-GIF) eluted in DEAE anion-exchange chromatography at a similar ionic strength (0.2 M NaCl) to human GIF (h-GIF) [1] and gave single electrophoretic bands at identical positions in both non-denaturingand SDS-PAGE. They eluted with the same apparent molecular weight as Cd_7-MT-2 from rat liver on gel filtration (data not shown). The masses of b-GIF apo-protein and of e-GIF S-methylated apo-protein were 6,975 and 7,250 Da, respectively. These values correspond to those calculated from the amino acid sequences (see below). Yields of both b-and e-GIFs obtained from a number of brain isolations ranged between 2–4 μg/g of tissue. The addition of 20 μg/ml of native Cu,Zn-GIFs to slice cultures of rat hippocampus induced neuronal degeneration after a three-day period. However, no effect was detected when 2 μg/ml of GIF was added.

The amino acid sequences of b- and e-GIF are shown in Table 1. The N-terminal Met in both sequences is blocked by an acetyl group (Ac) similarly to those of vertebrate MTs but e-GIF preparations also contained a variable amount of the non-acetylated protein. By comparing the e-GIF and b-GIF primary structures with those of h-GIF, m-GIF and r-GIF, a consensus GIF

TABLE 1 Amino acid sequences of GIFs and structurally-characterized MTs.

		1 5 10 15 20 25 30 35 40 45 50 55 60 65 70
		. . . .
Consensus	GIF[a]	Ac-MDPETCPCPTGGSCTCSDKCKCKGCKCTSCKKSCCSCCPAECEKCAKDCVCKGGEGAEAEAEKCSCCQ
Bovine	GIF	Ac-MDPETCPCPTGGSCTCSDPCKCEGCTCASCKKSCCSCCPAECEKCAKDCVCKGGEGAEAEEKKCSCCQ
	Trypsin[b] MS/MS	——— ——— ——— ——— ——— ——— ——— ———
Equine	GIF	Ac-MDPETCPCPTGGSCTCSGECKCEGCKCTSCKKSCCSCCPAECEKCAKDCVCKGGEGAEAEAEKCSCCQ
	Trypsin Acid	——— ——— ——— ——— ——— ——— ——— ———
Human	GIF[c]	X-MDPETCPCPSGGSCTCADSCKCEGCKCTSCKKSCCSCCPAECEKCAKDCVCKGGEAAEAEAEKCSCCQ
Mouse	GIF[d]	MDPETCPCPTGGSCTCSDKCKCKGCKCTNCKKSCCSCCPAGCEKCAKDCVCKGEEGAKAEAEKCSCCQ
Rat	GIF[e]	MDPETCPCPTGGSCTCSDKCKCKGCKCTNCKKSCCSCCPAECEKCAKDCVCKGEEGAKAE__KCSCCQ
Human	MT-2[f]	Ac-MDPN_CSCAAGDSCTCAGSCKCKECKCTSCKKSCCSCCPVGCAKCAQGCICK_____GASDKCSCCA
Rat	MT-2[f]	Ac-MDPN_CSCATDGSCSCAGSCKCKQCKCTSCKKSCCSCCPVGCAKCSQGCICK_____EASDKCSCCA
Rabbit	MT-2a[f,g]	Ac-MDPN_CSCA$_A^A$GDSCTCANSCTCKACKCTSCKKSCCSCCPPGCAKCAQGCICK_____GASDKCSCCA

[a] Consensus amino acid at each point is taken as that which occurs most often in the 5 GIF sequences. [b] Bars represent peptides for which sequences have been determined. [c] Taken from [1]. [d] Taken from [4]. [e] Taken from [9]. [f] See [3] and references therein. [g] At position 10 $_A^A$ represents AA.

sequence was obtained (Table 1). Compared with mammalian MTs, GIFs contain 68 rather than 61 amino acid residues with inserts of a single Thr and an acidic hexapeptide in the N- and C-terminal regions, respectively. The GIF consensus sequence shows 65% sequence similarity with those of mammalian MTs, with the array of 20 Cys being preserved. The sequence of rat GIF is shorter by two amino acids at the C-terminus [5] (Table 1).

In spite of the sequence similarity between GIFs and MTs, the latter show no activity in neuronal cell culture [1] suggesting significant differences in their three-dimensional structures. The spatial structures of mammalian $Me(II)_7$-MTs from rat, rabbit and human exhibit an identical molecular architecture [17]. Hence, analysis of the differences between the GIF consensus sequence and these MT sequences may provide insight into the structure of GIF (Table 1). The insertion of a hexapeptide between residues 52 and 53 relative to the MT sequences occurs in the region of the third exon which, in the spatial structures of mammalian $Me(II)_7$-MTs, encompasses the $Me(II)_4(CysS)_{11}$ cluster domain (α-domain) [2]. In these structures two 3_{10} helical segments are found between residues 41–45 and 57–61. Although the inserted amino acid sequences are not fully conserved among GIFs, their compositions suggest a propensity for helical structure. Thus, a large stretch of helical structure may develop in the C-terminal region of GIF. The N-terminal domain (β-domain) of $Me(II)_7$-MTs encompasses the $Me(II)_3(CysS)_9$ cluster. In the GIF sequences, besides the insertion of a single Thr at position 5, there are several conservative replacements in the N-terminal region. Compared with MT, major differences in the structure of GIF are expected between residues 4–12, due mainly to the presence of 2 Pro, each flanking a Cys (Table 1). As Pro is known to promote formation of β-conformation in proteins [18], the conserved Met(1)-Asp-Pro-Glu-Thr-Cys-Pro-Cys-Pro(9) sequence in GIFs is predicted to contain additional turns. Moreover, the occurrence of two non-bulky Gly at positions 11 and 12 would allow a substantially more tightly-folded structure to be formed in this region (Table 1). Pro-rich regions, such as that found in the N terminus of GIF, commonly occur in binding domains of salivary proteins, transcription factors, immunoglobulins etc. [18]. Indeed, inspection of the Swissprot and GenEMBL sequence databases revealed that the Cys-Pro-Cys-Pro repeat sequence is found in a number of receptor-like and transcription-regulating proteins. This may have relevance for the neuronal growth inhibitory activity of GIF.

Table 2
Metal stoichiometries of the isolated GIF proteins

Species	mol Cu/mol protein	mol Zn(Cd)[a]/mol protein
Human[b]	4	3
Bovine	0.9 ± 0.1 (4)[c]	4.4 ± 0.1 (3)
Equine	2.6 ± 0.2 (4)	2.1 ± 0.4 (2)

[a]The native zinc stoichiometries of b- and e-GIF are based on the cadmium contents of the respective Cd-derivatives. [b]Taken from [1]. [c]Number of separate preparations.

The b-GIF and e-GIF proteins from 3–5 bovine or equine brains all contained bound Cu and Zn or, after Cd treatment, Cu and Cd (Table 2). About 1 mol Cu/mol protein was found in b-GIF, between 2–3 Cu/protein in e-GIF (Table 2) and 4 Cu/protein in h-GIF [1]. Although no changes in Cu content were detected during the course of Cu,Zn-GIF or Cu,Cd-GIF isolations, a substantial decrease in the Zn content was observed. This indicates that, unlike those of MT, the Zn(II) ions in GIF are rather labile. The protein-bound Cu could be released only upon treatment with the chelating agent DTC (see below). In MTs, the isostructural replacement of Zn(II) ions by the more strongly bound Cd(II) in vitro has been demonstrated [19]. Hence, the b- and e-Cu,Cd-GIF derivatives would provide a better estimate of the original Zn contents in these proteins. b-GIF contains about 5 mol Cd/mol protein, whereas e-GIF contains approximately 3 mol Cd/mol protein. Thus, native GIFs contain: bovine, 5 Zn: 1 Cu; equine, 3 Zn: 3 Cu; and human, 3 Zn: 4 Cu [1]. These compositions, which appear to be species-specific, differ from those in MTs where 7 divalent Zn(II) and/or Cd(II) and up to 14 monovalent Cu(I) ions can be bound.

3.2. Spectroscopic characterization

The absorption and circular dichroism (CD) studies were conducted on b-Cu_1Cd_5-GIF and e-Cu_3Cd_3-GIF. Their absorption spectra (Fig. 1, top left) are of a similar shape with a tailing to 330 nm. Lowering the pH to 2.0 releases the Cd(II) ions from the protein and the high-energy shoulder at about 250 nm disappears. By analogy with similar studies of Cd_7-MT we attribute the origin of this feature to CysS-Cd(II) charge-transfer transitions [20]. The spectrum of e-Cu,Zn-GIF is shown as an inset in Fig. 1. Based on the same argument, the shoulder at about 230 nm originates from CysS-Zn(II) charge-transfer transitions [20]. The low-energy shoulder at about 275 nm is present in all absorption spectra at both neutral and low pH values and corresponds to that expected for CysS-Cu(I) charge-transfer transitions. In both instances, based on metal determination after desalting, Cu was still bound to the protein. Similar properties have been reported for Cu(I)-MTs, where Cu(I)-thiolate coordination is well established [8,21], suggesting that Cu in GIFs is also bound by Cys thiolate ligands. No absorption above 250 nm was observed in the metal-free GIFs treated with the chelating agent DTC. The CD spectra of Cu,Cd-GIFs at pH 7.6 and pH 2 (Fig. 1, bottom left) show CD features below 250 nm which reflect the contributions from both the secondary structure of the polypeptide chain and optically active high-energy ligand to

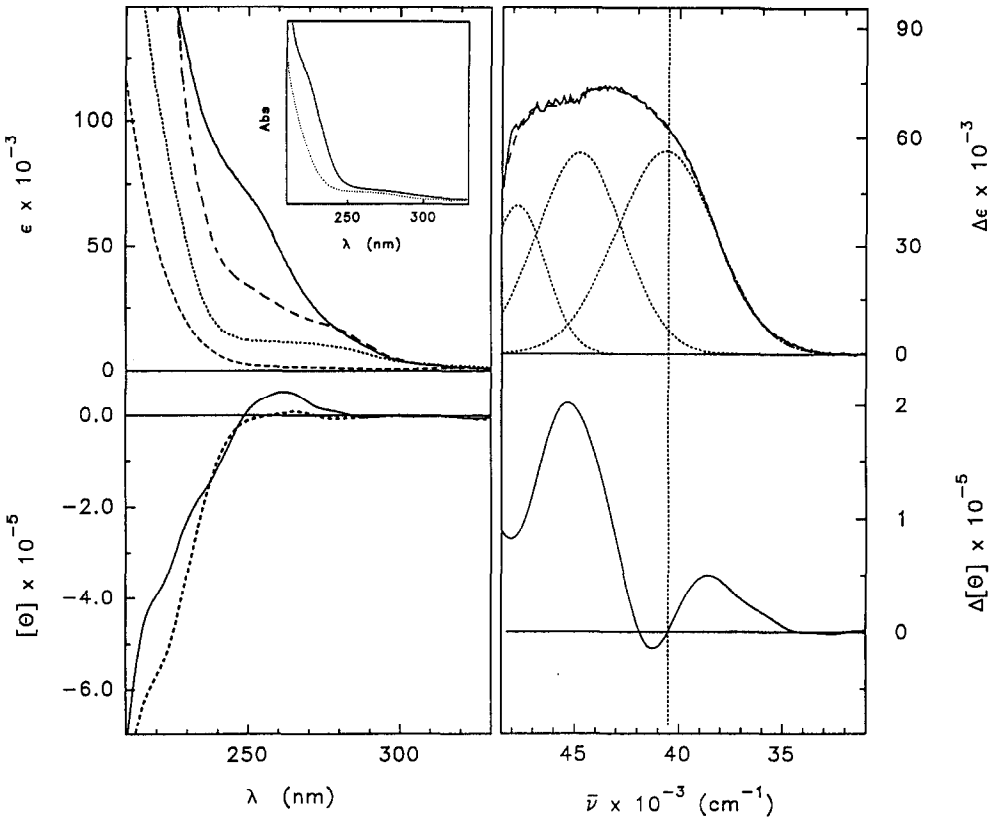

Fig. 1. Left panel: (Top) Absorption spectra of bovine Cu_1Cd_5-GIF (solid line) and equine Cu_3Cd_3-GIF (long-dashed line) at pH 7.6, bovine Cu_1-GIF (dotted line) and apo-GIF (dashed line) at pH 2. (Inset) Equine Cu,Zn-GIF (solid line) at pH 7.6 and Cu-GIF (dotted line) at pH 2. (Bottom) CD spectra of bovine Cu_1Cd_5-GIF (solid line) and Cu_1-GIF (dotted line). Right panel: Difference absorption (top) and CD (bottom) spectra of bovine Cu_1Cd_5-GIF vs. Cu_1-GIF. (Top) The Gaussian analysis of the difference absorption envelope with individual component bands (dotted line) and the overall fit (dashed line).

metal charge-transfer (LMCT) transitions. The CD bands above 250 nm represent a combination of overlapping lower-energy LMCT transitions of the Cd(II)-CysS and Cu(I)-CysS centers (see above). As with absorption, the spectra at pH 2 with CD bands at (+) 265 and (−) 280 nm originate only from the Cu(I)-thiolate LMCT bands, like those of Cu(I)-MTs [8,21].

Analysis of the similarily-shaped difference absorption and CD spectra of b- and eGIF (pH 7.6 vs. pH 2.0) affords information concerning organization of the Cd(II) sites. The representative difference absorption spectrum of b-Cu,Cd-GIF (Fig. 1, right panel) shows a broad band with a shoulder at 250 nm (ε = 60,000 $M^{-1} \cdot cm^{-1}$) and a maximum at about 230 nm. The number of Cys ligands involved in Cd-coordination can be determined, since it is linearly correlated with the difference absorption intensity of the low-energy feature [22]. Based on ε_{250} of about 5,500 $M^{-1} \cdot cm^{-1}$ per CysS ligand the 5 Cd(II) ions in b-Cu_1,Cd_5-GIF are coordinated by about 11–12 Cys, yielding a thiolate/Cd(II) ratio of between 2.2 to 2.4 and for e-Cu_3,Cd_3-GIF the 3 Cd(II) ions are coordinated by 7–8 Cys, i.e. thiolate/Cd(II) of about 2.5. In Cd7-MT, where tetrahedral tetrathiolate metal coordination by both terminal and bridging thiolate ligands is present, the thiolate/Cd ratios are 3 and 2.75 for the 3-metal and 4-metal cluster, respectively [2]. Gaussian analysis of the difference absorption envelope reveals at least three bands, which suggests the presence of at least three overlapping CysS-Cd(II) charge-transfer transitions. Whereas a close correspondence between the second Gaussian band at 225 nm and the difference CD band at 223 nm exists, at the position of the first Gaussian band at 247 nm two oppositely-signed CD bands at (+) 260 and (−) 242 nm with a cross-over point at the absorption maximum are observed (Fig. 1, right panel). Similar behaviour in the CD studies of Cd_7-MTs has been assigned to excitonic coupling of CysS-Cd(II) charge-transfer transitions within the cluster structures [23]. Thus, Cd(II)-CysS clusters should be present in both b- and e-Cu,Cd-GIFs.

Evidence that Cu is bound to b- and e-GIF as the cuprous ion is provided by their luminescence spectra (data not shown). The emission spectra of both b- and e-Cu,CdGIF at 77 K exhibit broad bands with maxima at 550 and 590 nm, respectively, each with shoulders at about 700 nm. The large Stokes' shifts and long life-times (100 μs) of these bands are consistent with emissions from triplet excited states. Such features, typical of Cu(I)

complexes, have been observed with Cu(I)-MTs [8], which exhibit principal emission bands at about 600 nm with slightly longer life-times relative to GIFs of around 130 μs [8]. Thus, spectroscopic properties of copper in GIFs indicate the presence of Cu(I)-thiolate complex(es).

In summary, our results show that: (i) both Cu and Zn are always present in GIF and are presumably both functionally important; (ii) Cu is incorporated in speciesspecific ratios and is present as the Cu(I) ion coordinated by Cys; (iii) bound Zn is labile and organized in Zn(II)-CysS cluster(s).

Acknowledgements: The authors gratefully acknowledge R. Sack and H. Vodičková for technical assistance, Prof. B. Gähwiler for the slice culture studies and Prof. J.H.R. Kägi for helpful discussions. This work was supported by grants from the Swiss National Science Foundation No. 31-32572.91 and the Kanton of Zürich.

References

[1] Uchida, Y., Takio, K., Titani, K., Ihara, Y. and Tomonaga, M. (1991) Neuron 7, 337–347.
[2] Pountney, D.L., Kägi, J.H.R. and Vašák, M. (1994) in: Handbook on Metal-Ligand Interactions in Biological Fluids (Berthon, G., Ed.) Vol. 1, Marcel Dekker Inc., New York, in press.
[3] Kägi, J.H.R. (1993) in: Metallothionein III (Suzuki, K.T., Kimura, M. and Imura, N., Eds.) Birkhäser, Basel, 29–56.
[4] Palmiter, R.D., Findley, S.D., Whitmore, T.D. and Durnam, D.M. (1992) Proc. Natl. Acad. Sci. USA 89, 6333–6337.
[5] Tsuji, S., Kobayashi, H., Uchida, Y., Ihara, Y. and Miyatake, T. (1992) EMBO J. 11, 4843–4850.
[6] Pountney, D.L. and Vašák, M. (1992) Eur. J. Biochem. 209, 335–341.
[7] Ding, X.- Q., Butzlaff, C., Bill, E., Pountney, D.L. Henkel, G., Winkler, H., Vašák, M. and Trautwein, A.X. (1994) Eur. J. Biochem., 220, 827–837.
[8] Pountney, D.L., Schauwecker, I., Zarn, J. and Vašák, M. (1994) Biochemisty, in press.
[9] Tsuji, S., Kobayashi, H., Uchida, Y., Ihara, Y. and Miyatake, T. (1992) EMBO J. 11, 4843–4850.
[10] Tommey, A.M., Shi, J., Lindsay, W.P., Urwin, P.E. and Robinson, N.J. (1991) FEBS Lett. 292, 48–52.
[11] Uchida, Y. (1993) in: Metallothionein III (Suzuki, K.T., Kimura, M. and Imura, N., Eds.), Birkhäser, Basel, pp. 315–328.
[12] Hunziker, P.E. (1991) Methods Enzymol. 205, 451–452.
[13] Hunziker, P.E. (1991) Methods Enzymol. 205, 399–400.
[14] Hunziker, P.E. (1991) Methods Enzymol. 205, 421–426.
[15] Biemann, K. (1992) Annu. Rev. Biochem. 61, 977–1010.
[16] Gähwiler, B.H. and Knöpfel, T. (1990) in: Preparations of Vertebrate Central Nervous System In Vitro (Jahnsen, H., Ed.), Wiley, London, pp. 75–100.
[17] Braun, W., Vašák, M., Robbins, A.H., Stout, C.D., Wagner, G., Kägi, J.H.R. and Wüthrich, K. (1992) Proc. Natl. Acad. Sci. USA 89, 10124–10128.
[18] Williamson, M.P. (1994) Biochem. J. 297, 249–260.
[19] Messerle, B.A., Schäffer, A., Vašák, M., Kägi, J.H.R. and Wüthrich, K. (1992) J. Mol. Biol. 225, 433–443.
[20] Vašák, M., Kägi, J.H.R. and Hill, H.A.O. (1981) Biochemistry 20, 2852–2856.
[21] Li, Y.-J. and Weser, U. (1992) Inorg. Chem. 31, 5526–5533.
[22] Henehan, C.J., Pountney, D.L., Zerbe, O. and Vašák, M. (1993) Prot. Sci. 2, 1756–1764.
[23] Willner, H., Vašák, M. and Kägi, J.H.R. (1987) Biochemistry 26, 6287–6292.